

Article

New Margin-Based Biochar for Removing Hydrogen Sulfide Generated during the Anaerobic Wastewater Treatment

Younes Gaga¹, Safaa Benmessaoud^{1,*}, Mohammed Kara^{1,*} , Amine Assouguem^{2,3} , Abdullah Ahmed Al-Ghamdi⁴, Fahad M. Al-Hemaid⁴, Mohamed S. Elshikh⁴ , Riaz Ullah⁵ , Artur Banach⁶ and Jamila Bahhou¹

- ¹ Laboratory of Biotechnology, Conservation and Valorisation of Natural Resources (LBCVNR), Faculty of Sciences Dhar El Mehraz, Sidi Mohamed Ben Abdallah University, Fez 30000, Morocco
- ² Laboratory of Functional Ecology and Environment, Faculty of Sciences and Technology, Sidi Mohamed Ben Abdallah University, Fez 30000, Morocco
- ³ Laboratory of Applied Organic Chemistry, Faculty of Sciences and Technology, Sidi Mohamed Ben Abdallah University, Imouzzzer Street, Fez 30000, Morocco
- ⁴ Department of Botany and Microbiology, College of Science, King Saud University, Riyadh 11451, Saudi Arabia
- ⁵ Department of Pharmacognosy, College of Pharmacy, King Saud University, Riyadh 11451, Saudi Arabia
- ⁶ Department of Biology and Biotechnology of Microorganisms, Institute of Biological Sciences, Faculty of Natural Sciences and Health, The John Paul II Catholic University of Lublin, Konstantynów 1I Str., 20010 Lublin, Poland
- * Correspondence: safaa.benmessaoud@usmba.ac.ma (S.B.); mohammed.kara@usmba.ac.ma (M.K.)



Citation: Gaga, Y.; Benmessaoud, S.; Kara, M.; Assouguem, A.; Al-Ghamdi, A.A.; Al-Hemaid, F.M.; Elshikh, M.S.; Ullah, R.; Banach, A.; Bahhou, J. New Margin-Based Biochar for Removing Hydrogen Sulfide Generated during the Anaerobic Wastewater Treatment. *Water* **2022**, *14*, 3319. <https://doi.org/10.3390/w14203319>

Academic Editor: Yongchang Sun

Received: 11 September 2022

Accepted: 29 September 2022

Published: 20 October 2022

Publisher's Note: MDPI stays neutral with regard to jurisdictional claims in published maps and institutional affiliations.



Copyright: © 2022 by the authors. Licensee MDPI, Basel, Switzerland. This article is an open access article distributed under the terms and conditions of the Creative Commons Attribution (CC BY) license (<https://creativecommons.org/licenses/by/4.0/>).

Abstract: The present research concerns the development of a new device and process intended for the purification and treatment of sulfurous elements, and more particularly, of hydrogen sulfide (H₂S) from the biogas produced at the time of the anaerobic fermentation in the purification stations. The controlled dumps or any other unit are likely to produce biogas with concentrations of H₂S harmful to the operation of the machines for the valorization of the produced biogas or deodorization. This device uses new biochar from a mixture of dehydrated digested sludge from sewage treatment plants and margins from traditional crushing units, followed by biological treatment in a liquid medium at a controlled temperature. The liquid medium is based on a margin (nutrient) with culture support (large granules of biochar) in suspension by the injection under the pressure of biogas coming from the biochar filter. Physico-chemical characterization of the biochar and a test practiced on the new device of raw biogas treatment were realized. The results showed that the newly synthesized biochar has a low specific surface and a highly undeveloped porosity. The spectrum corresponding to the images of the biochar reveals the presence of C, O, N, Al, Si, P, and Fe, as significant elements with the following respective percentages: 37.62%, 35.78%, 1.87%, 4.26%, 7.33%, 8.56%, and 4.58%. It is important to note that the C content of the biochar thus synthesized found by EDX is quite comparable to that estimated from ATG. Biogas treatment test results on the prototype object of the invention eliminated 97% of the H₂S from the biogas produced.

Keywords: new device; purification; treatment of sulfurous; margin; biochar filter; treatment of sulfurous

1. Introduction

Increasing concerns about climate change, air quality, energy import dependence, and fossil fuel depletion are increasing the demand for renewable fuels. The production site of these renewable fuels is multiple: landfills, sewage treatment plants, and industrial or food waste treatment plants [1].

Biogas results from the anaerobic digestion of organic matter by a consortium of microorganisms. It is a removable energy mainly composed of methane (CH₄) and carbon

dioxide (CO₂). There are other gases such as nitrogen (N₂), water vapor (H₂O), ammonia (NH₃), hydrogen sulfide (H₂S), siloxanes, and other sulfur compounds.

The biogas must be cleaned (removal of H₂S and siloxanes) and upgraded (removal of CO₂) to be used as an energy source (biomethane) to produce heat and electricity [2]. H₂S in biogas is typically 50–5000 ppmv, but in some cases it can reach 20,000 ppmv (2% v/v). It is a colorless, flammable, and foul-smelling toxic gas.

This contaminant is known for its undesirable odor and is transformed into sulfur dioxide (SO₂) and sulfuric acid (H₂SO₄), which are highly corrosive and dangerous for health and the environment. Its elimination is essential for any possible use of biogas [3–5].

According to several authors, sewage sludge is a problematic waste and a valuable raw material for producing biogas and biochar by thermal conversion which is an environmentally friendly alternative [6–8].

Nevertheless, the biogas produced contains impurities that make its direct use in machines of valorization, either thermal or electric energy. Almost impossible or comes back to too expensive maintenance costs were to the necessity to purify the produced biogas of the sulfurous elements in general and the hydrogen sulfide H₂S, especially before its use. The operating costs and/or unpredictably high H₂S efficiencies [9–11].

The present article refers to the treatment and purification of anaerobic digestion gases. More particularly for a device, this is a process for purification and treatment of sulfurous elements in the biogas produced by anaerobic digestion, especially hydrogen sulfide H₂S.

“Biochar” is a recently coined term emerging in conjunction with renewable fuel and carbon sequestration. It is another carbon-based material that is produced by a combination of pyrolysis (limited amount of oxygen) and thermal degradation of organic material at temperatures between 100–700 °C [12–14]. Several recent types of research have worked on directly adding biochar to anaerobic digestion systems. Unfortunately, they have focused on improving CH₄ production but have not addressed the effect of biochar addition on H₂S production [15–17].

Shen et al. (2015) added corn stover-based biochar directly to an anaerobic digester treating municipal wastewater, resulting in biogas production with over 90% CH₄ and less than five parts per billion H₂S [18]. Another study used pine and white oak biochar in digesters to increase the percentage of CH₄ in the biogas stream [17].

Studies have been carried out on the development of a multifunctional, efficient, and durable membrane for long-term use in the treatment of complex oily wastewater [19,20]. To our knowledge, there is no study on using biochar formed from wastewater treatment plant sludge and margins for H₂S reduction.

The origin of this work concerns the development of a new device and process designed for the purification and treatment of sulfurous elements in biogas using sludge from the wastewater treatment plant and the margins as a source of biochar production.

The main objectives of this work involve:

- i. Valorizing sludge from sewage treatment plants and margins (source of pollution).
- ii. Reduction in the costs of consumables by using the mixture of sludge and margins as raw material to produce biochar as adsorbent.

2. Materials and Methods

2.1. Biochar Production

The slow pyrolysis produces the biochar in the absence of oxygen at a temperature between 400 and 500 °C for a minimum of 4 h, using a dried mixture of digested and dehydrated sewage plant sludge (80% dryness) with raw margins from the crushing of olive oil. After mixing the sludge and the margin, a second natural drying is carried out to bring the dryness of the mixture back to 80% before starting the pyrolysis to produce the biochar (final product, as shown in Figure 1) [21–23].



Figure 1. Image of biochar obtained by pyrolysis of a sludge–margin mixture at 500 °C.

2.2. Physicochemical Characterization of Biochar

Infrared (IR) spectroscopy was used to characterize the biochar. The IR spectra illustrate the bond stretches in the organic functional groups on the biochar surface [24].

The thermal stability of this material was identified by ATG thermogravimetric analysis with a heating rate of 10 °C/min up to a temperature of 800 °C under gas (nitrogen) sweep [25].

The pore size distribution and surface characteristics of the prepared biochar were measured by N₂ gas adsorption–desorption at the temperature of liquid N₂ (−195.85 °C). The Brunauer determined the specific surface areas—Emmett–Teller (BET) method. Inductively coupled plasma spectrometry was used for the characterization of inorganic constituents of the biochar sample. The analysis was used to identify the metals in the samples (Mg, Al, Si, P, Ca, Mn, Fe, Ni, Cu, Zn, Na, B, Co, Pb, and Cd) and to measure the content of these elements [26,27].

The surface morphology and distribution of the chemical elements of biochar were studied by scanning electron microscopy (SEM). SEM images of biochars were obtained using a Gemini SEM 500-8203017153 scanning electron microscope (SEM) with an accelerating voltage of 3.00 kV [28].

2.3. Description of the Pilot

Several pilots were set up during this experiment to test the H₂S adsorption capacities of the materials studied.

The whole device of desulfurization of the anaerobic digestion biogas by biochar filter and drowned reactor based on margin with suspension culture is formed of (Figure 2):

- ✓ A biochar filter (2) whose biochar is produced from a mixture of sewage plant sludge and margin used as an adsorbent for the pre-filtration of sulfur compounds in biogas and, more particularly, hydrogen sulfide (H₂S).
- ✓ Hydraulic guard (5) to ensure minimum hydraulic pressure through the biochar filter and can serve as an additional biological treatment reactor.

2.4. Statistical Analysis

To confirm our outcome reliability and reproducibility, we compared the mean values of each parameter (H₂S and CH₄) upstream and downstream for our anaerobic digestion biogas desulfurization system by biochar filter, using the two-sample *t*-test at *p* < 0.05 with Minitab19.1.

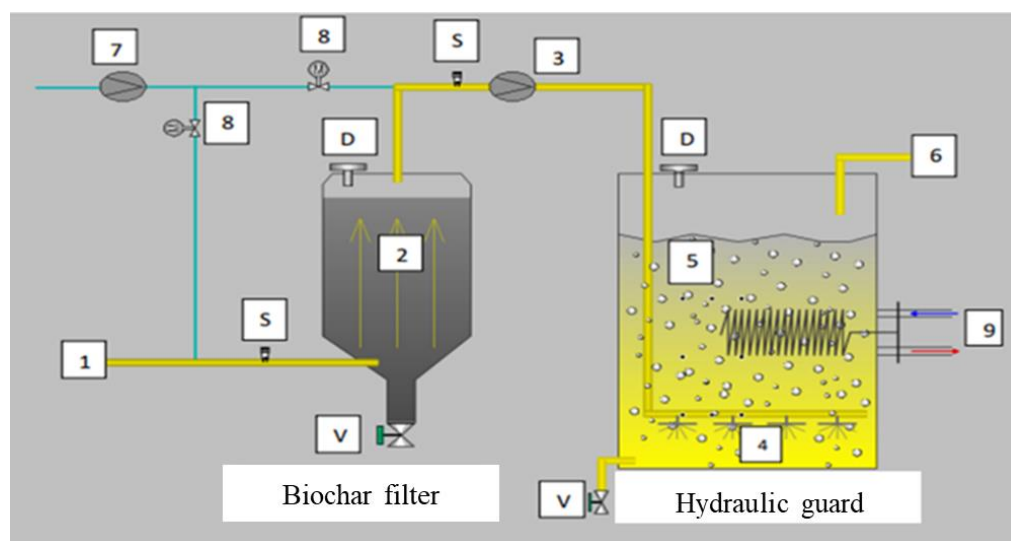


Figure 2. Overall drawing of the anaerobic digestion biogas desulfurization system by biochar filter and liquid margin suspension culture reactor: 1: raw biogas inlet; 2: biochar filter; 3: biogas injection system under pressure; 4: pressurized biogas diffusers; 5: Hydraulic guard; 6: cleaned biogas outlet to use; 7: oxygen injection system; 8: oxygen control valves in the biogas; 9: heat exchanger; S: oxygen control probes; D: nutrient injection point (margin or others; V: Purge or drain valve.).

3. Results and Discussion

Physicochemical Characterization of Biochar

The type of functional groups present on the surface of the biochar is crucial because they generally improve its adsorption abilities. Indeed, the presence of specific functional groups such as hydroxyl groups or the presence of water in the biochar favors the formation of an aqueous film on the surface of the biochar allowing the dissociation of hydrogen sulfide into HS. The IR spectrum of the biochar is shown in Figure 3. Several bands characteristic of different groups can be distinguished (Figure 3a).

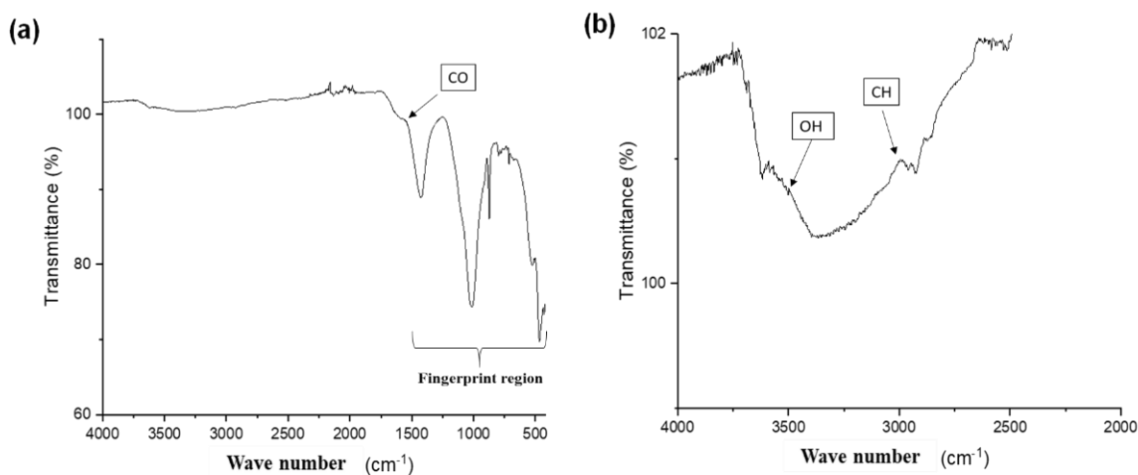


Figure 3. (a) The infrared spectrum of biochar synthesized by pyrolysis of the sludge–margin mixture, (b) infrared spectrum of biochar synthesized in the region of wave numbers between 4000 and 2000 cm^{-1} .

A band located at 3365 cm^{-1} , characteristic of the elongation of O-H bonds, can be observed on the infrared spectrum (Figure 3b). This band of weak intensity informs the number of hydroxyl groups on the surface. It has been previously found that many free hydroxyl groups and structural hydroxyl groups (-COOH and -COH) decompose during the pyrolysis of the sludge [29]. Indeed, the mass loss found in a temperature range below

200 °C was only 3%, indicating the low water content of the material. The band observed at 2923 cm^{-1} is characteristic of elongations of aliphatic C-H bonds, while the band observed at 1794 cm^{-1} indicates the presence of carbonyl groups on the biochar surface. The intense band observed at 1427 can be attributed to C-H bond deformations. It is well established that the region between 400 cm^{-1} and 1500 cm^{-1} in an IR spectrum is known as the fingerprint region. It usually contains many peaks, making it difficult to identify individual peaks. However, the fingerprint region of a given compound is unique and, therefore, can be used to distinguish between compounds.

From the ICP results, we found that the material is composed of several elements such as Ca, P, Al, and Si, at a level greater than 20%. These elements are likely to form stable mineral phases at high temperatures, so an exact assignment of the different peaks observed on the infrared spectrum in the fingerprint region becomes difficult due to the complex composition of the biochar.

Thermogravimetric analysis was used to evaluate the thermal stability of the synthesized biochar. The thermogravimetric analysis was performed under air by heating the biochar at 10 °C/min to 800 °C. Figure 4 shows a mass loss of about 3% at a temperature of about 200 °C. This first mass loss corresponds to the dehydration of the biochar or decomposition of the oxygenated groups present on the material's surface. The mass loss observed after 200 °C, of 29%, corresponds to the decomposition and degradation of impurities, volatile matter, and carbon, mainly into CO and CO₂. The total mass loss found for the biochar is in the order of 33%, indicating that the carbon content of the material is relatively low. Therefore, the residue of 67% remaining at 800 °C indicates the presence of mineral phases that form under air at 800 °C. The results concerning the thermal stability of biochar, obtained by pyrolysis of a mixture of sludge and margin, are comparable to that of biochar obtained by pyrolysis of pigeon pea stems at 600 °C [30].

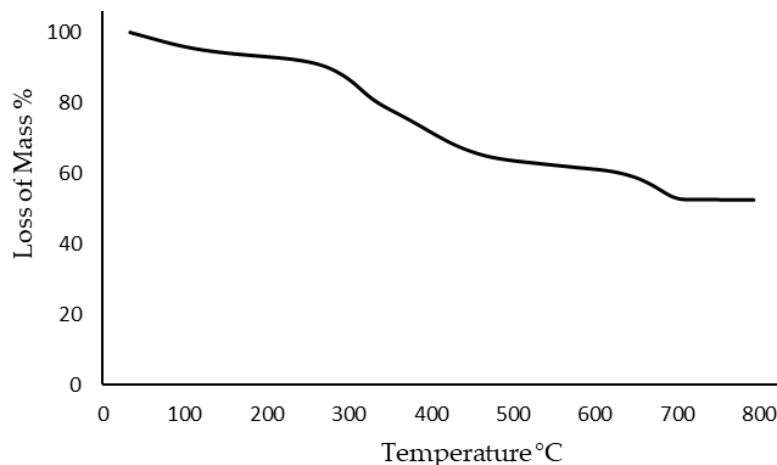


Figure 4. ATG curve of biochar synthesized by pyrolysis of a mixture of sludge and margins.

In order to identify the composition of the biochar and the different mineral phases likely to have been formed after the thermogravimetric analysis at 800 °C, we used ICP. Table 1 shows all biochar's metallic and non-metallic elements and their concentrations. This table also compares the attention of the features in the biochar to the allowable levels of contaminants in biochar as defined by the International Biochar Initiative (IBI), the British Biochar Foundation (BQM), and the European Biochar Foundation (EBC) [31].

Table 1. Permissible content of contaminants in biochar, based on the existing quality standard (IBI: International Biochar Initiative; BQM: British Biochar Foundation; EBC: European Biochar Foundation).

Element	Concentration Found for Synthesized Biochar (mg/kg)	Limit Value According to the Standard		
		IBI	BQM	EBC
B	42	-	-	-
Na	890	-	-	-
Mg	16.506	-	-	-
Al	21.345	-	-	-
Si	658	-	-	-
P	21.408	-	-	-
Ca	144.651	-	-	-
Mn	346	-	-	-
Fe	16.464	-	-	-
Co	5	-	-	-
Ni	33	47–420	10	30
Cu	727	143–6000	40	100
Zn	1315	416–7400	150	400
As	0	13–100	10	13
Cd	4.9	1.4–39	3	1
Pb	117	121–300	60	120

The results obtained from the ICP analysis show that the biochar contains high concentrations of Ca, Mg, Al, P, and Fe. The majority of elements comprising the biochar are calcium, with 14%, followed by phosphorus and aluminum, with percentages of about 2.14% and 2.13%, respectively. The biochar being rich in mineral elements and heteroatoms such as P and B explains the subsistence of a residue of about 67% after calcination under air at 800 °C. The high Ca content of the biochar can be explained by the liming of the sludge generally carried out to stabilize it.

The synthesized biochar has a dense structure, and no porosity can be appreciated at different magnifications (Figure 5a–c). By grinding the biochar, particles of the order of 17 µm in size were obtained (Figure 5b). Furthermore, at magnifications on the order of ×11,500, the material appears to possess a rough structure, probably due to mineral phase aggregates. The composition of the material was determined by energy dispersive X-ray spectroscopy (EDS). In Figure 5k, the spectrum corresponding to the biochar images reveals the presence of C, O, N, Al, Si, P, and Fe, as the majority elements with the following respective percentages: 37.62%, 35.78%, 1.87%, 4.26%, 7.33%, 8.56%, and 4.58%. It is important to note that the C content of the synthesized biochar found by EDX is quite comparable to that estimated from GTA. The SEM-EDS images of the biochar (Figure 5d–j) reveal the homogeneous distribution of the different elements on the biochar surface.

The exact composition of sludge varies according to the origin of the wastewater, the time of year, and the type of treatment and conditioning practiced in the treatment plant. The waste sludge represents, above all, a raw material composed of different elements (organic matter, fertilizing elements (N and P), metallic trace elements, organic trace elements, and pathogens) [32].

The concentration of organic matter can vary from 30 to 80%. The organic matter of the sludge is constituted by particles that have been eliminated by gravity. Lipids represent 6 to 19% of the organic matter, polysaccharides, proteins, and amino acids represent up to 33% of the organic matter. Thus, we find the products of metabolization and microbial bodies resulting from biological treatments (digestion, stabilization) [31].

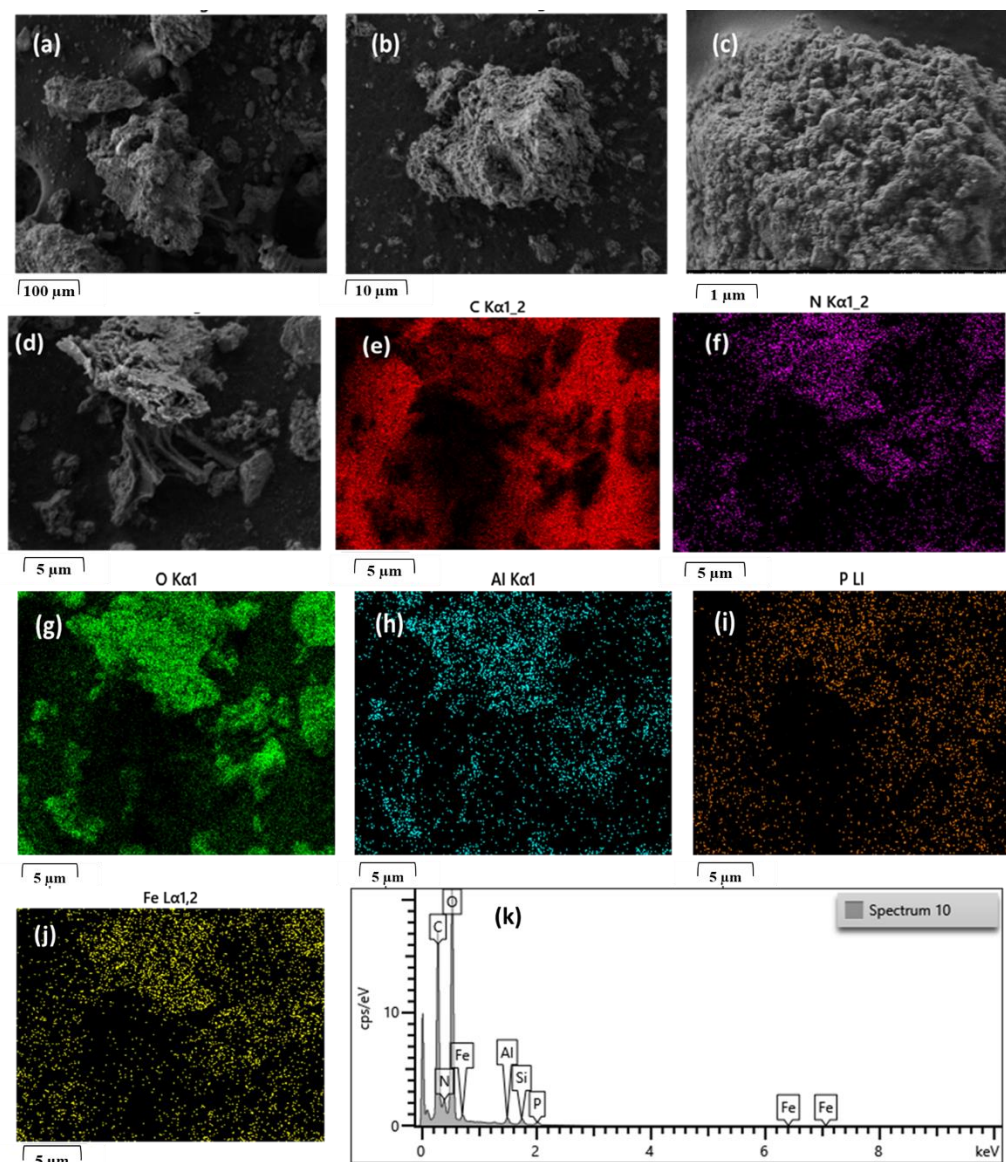


Figure 5. (a–c) SEM images of biochar; SEM image (d) and elemental distribution of C (e), N (f), O (g), Al (h), P (i), Fe (j), and (k) EDS spectrum of biochar.

The nature and concentration of organic and inorganic pollutants in wastewater depend on the activities connected to the network [33]. Most of the chemical contamination comes from industrial discharges and, to a lesser extent, from domestic discharges (use of solvents, do-it-yourself waste, detergent) [34]. Due to the settling during treatment, these chemical contaminants are found in very high concentrations compared to wastewater.

The knowledge of the specific surface, the pore volume, and the pore size define the biochar structure. The ability of these properties is of great importance because they help to explain the accessibility of the surface to adsorbates related to the shape and size of the pores and, consequently, its adsorption ability. The nitrogen adsorption isotherm is plotted by plotting the amount adsorbed per gram of adsorbent against relative pressure. The nitrogen adsorption curve for biochar is shown in Figure 6. From the figure, it can be seen that the isotherm obtained for the biochar is type II. Type II isotherms are typically received on non-porous or macroporous materials, where monolayers and multilayers form on the surface [35].

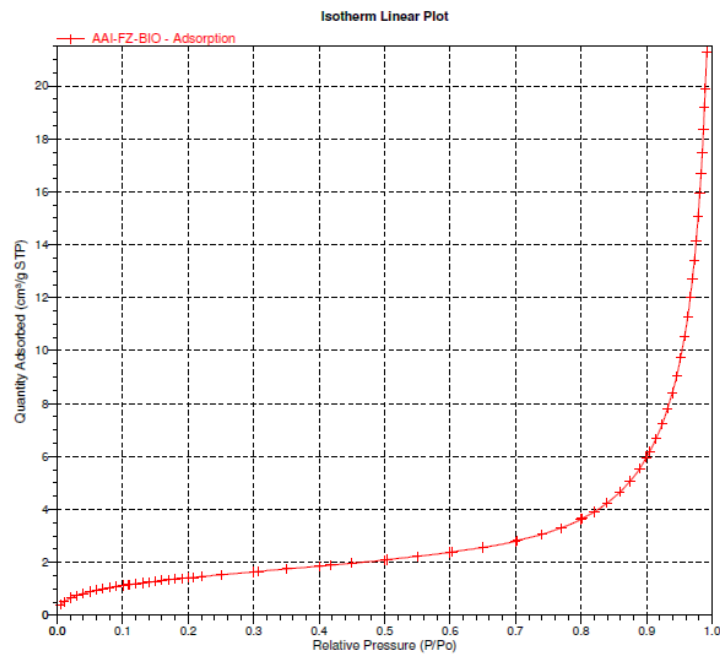


Figure 6. Adsorption isotherm of the prepared biochar.

The result obtained is in perfect agreement with the scanning electron microscopy. Indeed, in the SEM pictures, we noticed that the material does not present any porosity and that the observed structure is relatively dense. The synthesized biochar has a low specific surface and a highly undeveloped porosity explaining the obtaining of a type II isotherm characteristic of materials with no porosity.

From the results of monitoring the biogas treatment in a device, it is found that the concentration of hydrogen sulfide in the raw biogas is 5000 ppm upstream. Moreover, this biogas downstream of the treatment device is about 131 ppm after 38 days of treatment (Figure 7).

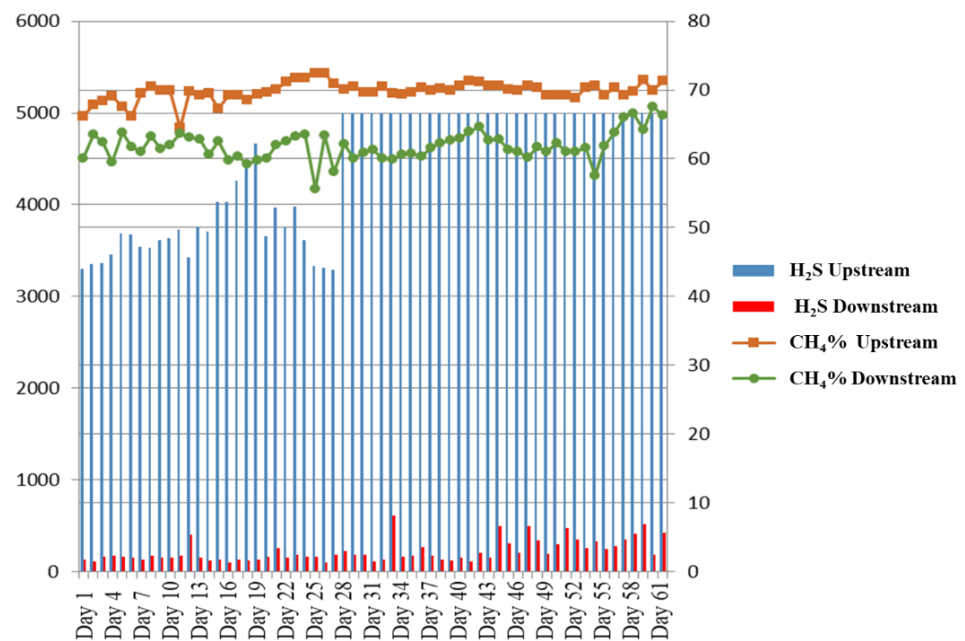


Figure 7. Graphic presentation of the biogas treatment test results on the prototype object of the invention.

A study was carried out on H₂S adsorption with non-hazardous waste incineration bottom ash and was mainly studied with natural biogas. The reactors were more significant than those used for biochars, and the experiments lasted longer. Adsorption capacities ranged from 3 to 298 mgH₂S/g material. The lowest value was obtained with dry biogas, and 15% moistened MIDND.

The flow rate necessary for the sizing of the biochar filter, and in order to have the targeted results (minimum abatement of 90%) for a raw biogas concentration of 5000 ppm of hydrogen sulfide, is 0.5 m³/h of biogas for a biochar volume of 30 L and a volume of 20 L for the biological reactor for the same flow rate.

The results shown in Figure 8 represent the comparison between the average values of each parameter of H₂S and CH₄ in the anaerobic digestion biogas desulphurization system upstream and downstream by the BIOCHAR filter. The (Figure 8A) shows a crucial decrease in the amount of H₂S between the front and back of our system ($p < 0.05$). While the amount of CH₄ shows no difference between upstream and downstream (Figure 8B). This difference allows us to confirm the efficiency of our prototype in reducing the hydrogen sulfide generated during the anaerobic wastewater treatment.

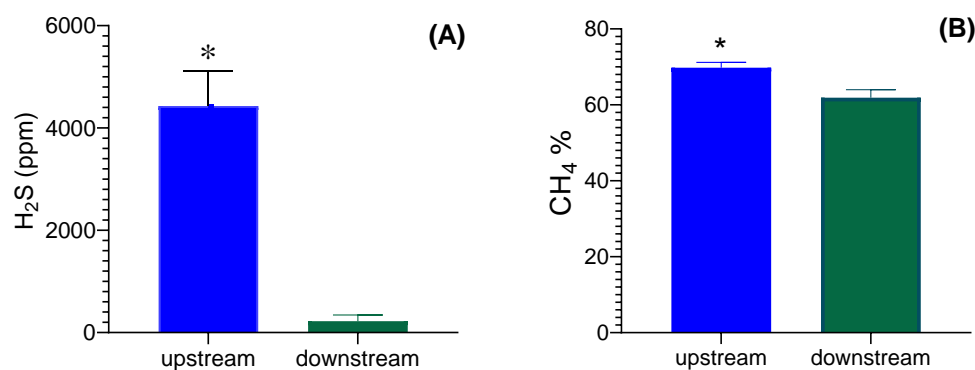


Figure 8. Graphic presentation of the comparison between the mean values of each parameter: (A) H₂S, (B) CH₄ (upstream and downstream). * The two means in the same graph are significantly different (*t*-test, $p < 0.05$).

The particularity of this device and process is that it allows treating a wide range of biogas produced in anaerobic digestion systems while ensuring highly efficient yields with short residence times, valorizing the harmful by-products coming from the sewage treatment plants (sludge) and the crushing of olives (margin), posing problems for the sewage treatment plants and for the natural environment. This allows the minimizing of the expenses on the consumables used in the prior art processes, activated carbons, minerals, and nutrients for the biomass with easy exploitation for maximum safety.

Biochar used in this study was rich in mineral elements. It is likely that the minerals in the biochar contribute to H₂S removal. Mineral content (from EDS analysis) and speciation (from ICP-OES analysis) are essential factors to consider, as metal oxides such as Ca, Mg, Al, and Fe and other elements such as P can act as H₂S adsorption sites and catalytic oxidation to convert H₂S to elemental sulfur and sulfates. This mainly explains the observed abatement rates and H₂S removal ability by the biochar used [36]. Indeed, studies on biochar substrates prepared from anaerobically digested sewage sludge and fiber have highlighted the importance of surface alkalinity in H₂S removal, as the alkaline nature was suspected to facilitate H₂S dissociation [37].

Several studies have been carried out on H₂S absorption using processes for removing hydrogen sulfide species from biogas by a carbon absorption material produced from dewatered and dried sewage sludge by adding mineral oil before pyrolysis. Adding mineral oil is an extra step compared to the biochar production process and an additional charge that will increase the cost of the product with a lower abatement rate than that

obtained by our device [38,39]. Even heat treatment alone is not sufficient for preparing a carbon absorbent.

In our study, we succeeded in combining the filtration of biogas doped with 2 to 5% oxygen on biochar support produced from a mixture of digested and dehydrated sewage sludge and margins from a traditional crushing unit. Followed by biological treatment in liquid medium at controlled temperature, the medium is based on margin (nutrient) with culture support (large granule of biochar) in suspension by the injection under the biogas pressure from the biochar filter.

The flooded reactor for the biological treatment of sulfur compounds in biogas is an innovation; the reactor is a mixture of diluted margin and culture media for the purifying biomass at adjustable temperature. The bubbling ensures the biomass's suspension and the medium's agitation due to the biogas injected under pressure at the bottom of the flooded biological reactor.

The bacterial flows in suspension fixed on the granules of biochar (suspension support) ensure the elimination is ensured after that. The nutrition of this biomass is brought by the margin, which is the base of the solution of the biological reactor (the use of conventional nutrients is also possible); the final product is biogas in conformity with use.

4. Conclusions

A new adsorption process for hydrogen sulfide removal from biogas by margin-based biochar was tested on a pilot scale. Results showed that this biochar is characterized by a dense and mineral-rich structure. It is likely that these biochar minerals can act as H₂S adsorption and catalytic oxidation sites to convert up to 98% of the H₂S to elemental sulfur and sulfates.

The process has shown promise and further experimental work is underway to refine the new treatment device, which will be investigated, and reported in a subsequent publication.

Author Contributions: Conceptualization, Y.G., S.B. and J.B.; Data curation, A.A., R.U. and M.S.E.; Formal analysis, M.K., A.A. and M.S.E.; Investigation, Y.G., S.B. and J.B.; Methodology, Y.G., S.B., M.K., A.A. and J.B.; Software, M.K., A.A. and A.B.; Supervision, J.B.; Writing—original draft, Y.G., S.B. and J.B.; Writing—review & editing, Y.G., S.B., M.K., R.U., F.M.A.-H., A.A., A.A.A.-G. and A.B. All authors have read and agreed to the published version of the manuscript.

Funding: The authors extend their appreciation to the Researchers Supporting Project number (RSP2022R483), King Saud University, Riyadh, Saudi Arabia.

Data Availability Statement: Not applicable.

Acknowledgments: The authors extend their appreciation to the Researchers Supporting Project number (RSP2022R483), King Saud University, Riyadh, Saudi Arabia.

Conflicts of Interest: The authors declare no conflict of interest.

References

1. Rasi, S.; Läntelä, J.; Rintala, J. Trace Compounds Affecting Biogas Energy Utilisation—A Review. *Energy Convers. Manag.* **2011**, *52*, 3369–3375. [[CrossRef](#)]
2. Hong, J.; Hong, J.; Otaki, M.; Jolliet, O. Environmental and Economic Life Cycle Assessment for Sewage Sludge Treatment Processes in Japan. *Waste Manag.* **2009**, *29*, 696–703. [[CrossRef](#)]
3. Abatzoglou, N.; Boivin, S. A Review of Biogas Purification Processes. *Biofuels Bioprod. Biorefining* **2009**, *3*, 42–71. [[CrossRef](#)]
4. Rangabhashiyam, S.; dos Santos Lins, P.V.; de Magalhães Oliveira, L.M.; Sepulveda, P.; Ighalo, J.O.; Rajapaksha, A.U.; Meili, L. Sewage Sludge-Derived Biochar for the Adsorptive Removal of Wastewater Pollutants: A Critical Review. *Environ. Pollut.* **2022**, *293*, 118581. [[CrossRef](#)]
5. Ben Ayed, R.; Moreau, F.; Ben Hlima, H.; Rebai, A.; Ercisli, S.; Kadoo, N.; Hanana, M.; Assouguem, A.; Ullah, R.; Ali, E.A. SNP discovery and structural insights into OeFAD2 unravelling high oleic/linoleic ratio in olive oil. *Comput. Struct. Biotechnol. J.* **2022**, *20*, 1229–1243. [[CrossRef](#)]
6. Fan, S.; Tang, J.; Wang, Y.; Li, H.; Zhang, H.; Tang, J.; Wang, Z.; Li, X. Biochar Prepared from Co-Pyrolysis of Municipal Sewage Sludge and Tea Waste for the Adsorption of Methylene Blue from Aqueous Solutions: Kinetics, Isotherm, Thermodynamic and Mechanism. *J. Mol. Liq.* **2016**, *220*, 432–441. [[CrossRef](#)]

7. Assouguem, A.; Kara, M.; Mechchate, H.; Al-Mekhlafi, F.A.; Nasr, F.; Farah, A.; Lazraq, A. Evaluation of the Impact of Different Management Methods on *Tetranychus urticae* (Acari: Tetranychidae) and Their Predators in Citrus Orchards. *Plants* **2022**, *11*, 623. [CrossRef]
8. Li, J.; Yu, G.; Pan, L.; Li, C.; You, F.; Wang, Y. Ciprofloxacin Adsorption by Biochar Derived from Co-Pyrolysis of Sewage Sludge and Bamboo Waste. *Environ. Sci. Pollut. Res.* **2020**, *27*, 22806–22817. [CrossRef]
9. Singh, S.; Kumar, V.; Dhanjal, D.S.; Datta, S.; Bhatia, D.; Dhiman, J.; Samuel, J.; Prasad, R.; Singh, J. A Sustainable Paradigm of Sewage Sludge Biochar: Valorization, Opportunities, Challenges and Future Prospects. *J. Clean. Prod.* **2020**, *269*, 122259. [CrossRef]
10. Gasquet, V. H₂S Removal from Biogas Using Raw and Formulated Thermal Treatment Residues: Performance Comparison and Understanding of Adsorption Mechanisms 2020. *Waste Biomass Valorization* **2020**, *11*, 5363–5373. [CrossRef]
11. Assouguem, A.; Kara, M.; Ramzi, A.; Annemer, S.; Kowalczyk, A.; Ali, E.A.; Moharram, B.A.; Lazraq, A.; Farah, A. Evaluation of the Effect of Four Bioactive Compounds in Combination with Chemical Product against Two Spider Mites *Tetranychus urticae* and *Eutetranychus orientalis* (Acari: Tetranychidae). *Evid. Based Complement. Altern. Med.* **2022**, *2022*, 2004623. [CrossRef] [PubMed]
12. Kambo, H.S.; Dutta, A. A Comparative Review of Biochar and Hydrochar in Terms of Production, Physico-Chemical Properties and Applications. *Renew. Sustain. Energy Rev.* **2015**, *45*, 359–378. [CrossRef]
13. Warnock, D.D.; Lehmann, J.; Kuyper, T.W.; Rillig, M.C. Mycorrhizal Responses to Biochar in Soil—Concepts and Mechanisms. *Plant Soil* **2007**, *300*, 9–20. [CrossRef]
14. Hale, S.; Hanley, K.; Lehmann, J.; Zimmerman, A.; Cornelissen, G. Effects of Chemical, Biological, and Physical Aging As Well As Soil Addition on the Sorption of Pyrene to Activated Carbon and Biochar. *Environ. Sci. Technol.* **2011**, *45*, 10445–10453. [CrossRef] [PubMed]
15. Jang, H.M.; Choi, Y.-K.; Kan, E. Effects of Dairy Manure-Derived Biochar on Psychrophilic, Mesophilic and Thermophilic Anaerobic Digestions of Dairy Manure. *Bioresour. Technol.* **2018**, *250*, 927–931. [CrossRef] [PubMed]
16. Meyer-Kohlstock, D.; Haupt, T.; Heldt, E.; Heldt, N.; Kraft, E. Biochar as Additive in Biogas-Production from Bio-Waste. *Energies* **2016**, *9*, 247. [CrossRef]
17. Shen, Y.; Linville, J.L.; Ignacio-de Leon, P.A.A.; Schoene, R.P.; Urgun-Demirtas, M. Towards a Sustainable Paradigm of Waste-to-Energy Process: Enhanced Anaerobic Digestion of Sludge with Woody Biochar. *J. Clean. Prod.* **2016**, *135*, 1054–1064. [CrossRef]
18. Shen, Y.; Linville, J.L.; Urgun-Demirtas, M.; Schoene, R.P.; Snyder, S.W. Producing Pipeline-Quality Biomethane via Anaerobic Digestion of Sludge Amended with Corn Stover Biochar with in-Situ CO₂ Removal. *Appl. Energy* **2015**, *158*, 300–309. [CrossRef]
19. Cao, W.; Ma, W.; Lu, T.; Jiang, Z.; Xiong, R.; Huang, C. Multifunctional Nanofibrous Membranes with Sunlight-Driven Self-Cleaning Performance for Complex Oily Wastewater Remediation. *J. Colloid Interface Sci.* **2022**, *608*, 164–174. [CrossRef]
20. Ma, W.; Jiang, Z.; Lu, T.; Xiong, R.; Huang, C. Lightweight, Elastic and Superhydrophobic Multifunctional Nanofibrous Aerogel for Self-Cleaning, Oil/Water Separation and Pressure Sensing. *Chem. Eng. J.* **2022**, *430*, 132989. [CrossRef]
21. Liu, C.; Jarochowska, E.; Du, Y.; Vachard, D.; Munnecke, A. Microfacies and Carbon Isotope Records of Mississippian Carbonates from the Isolated Bama Platform of Youjiang Basin, South China: Possible Responses to Climate-Driven Upwelling. *Palaeogeogr. Palaeoclimatol. Palaeoecol.* **2015**, *438*, 96–112. [CrossRef]
22. Effect of Process Parameters on Production of Biochar from Biomass Waste through Pyrolysis: A Review—ScienceDirect. Available online: https://www.sciencedirect.com/science/article/pii/S1364032115012010?casa_token=xRxhtKN9VeMAAAAA:STy7YFbCCGeuTirFgHpZFW5uul9SiQpRvcGRrjLKHl9CODoiqvnCXgfcP5DAHby6ZCHn2wfpTzyk (accessed on 23 July 2022).
23. Biochar: Production, Properties and Emerging Role as a Support for Enzyme Immobilization—ScienceDirect. Available online: https://www.sciencedirect.com/science/article/pii/S0959652620303140?casa_token=6_KadULQi5kAAAAA:hsTQ-M5a1MCd068PlsLPYnNQyYzATxkQ5jBE9r3sG9ZYusmwU7GTzemLIVq4yArEifwfCs0f4CI (accessed on 23 July 2022).
24. Younis, U.; Rahi, A.A.; Danish, S.; Ali, M.A.; Ahmed, N.; Datta, R.; Fahad, S.; Holatko, J.; Hammerschmidt, T.; Brtnicky, M.; et al. Fourier Transform Infrared Spectroscopy Vibrational Bands Study of *Spinacia Oleracea* and *Trigonella Corniculata* under Biochar Amendment in Naturally Contaminated Soil. *PLoS ONE* **2021**, *16*, e0253390. [CrossRef] [PubMed]
25. Qi, F.; Yan, Y.; Lamb, D.; Naidu, R.; Bolan, N.S.; Liu, Y.; Ok, Y.S.; Donne, S.W.; Semple, K.T. Thermal Stability of Biochar and Its Effects on Cadmium Sorption Capacity. *Bioresour. Technol.* **2017**, *246*, 48–56. [CrossRef] [PubMed]
26. Downie, A.; Crosky, A.; Munroe, P. Physical Properties of Biochar. In *Biochar for Environmental Management*; Routledge: London, UK, 2009; ISBN 978-1-84977-055-2.
27. Tan, Z.; Zou, J.; Zhang, L.; Huang, Q. Morphology, Pore Size Distribution, and Nutrient Characteristics in Biochars under Different Pyrolysis Temperatures and Atmospheres. *J. Mater. Cycles Waste Manag.* **2018**, *20*, 1036–1049. [CrossRef]
28. Gondim, R.S.; Muniz, C.R.; Lima, C.E.P.; Santos, C.L.A.D. Explaining the water-holding capacity of biochar by scanning electron microscope images. *Rev. Coatinga* **2018**, *31*, 972–979. [CrossRef]
29. Lu, H.; Zhang, W.; Wang, S.; Zhuang, L.; Yang, Y.; Qiu, R. Characterization of Sewage Sludge-Derived Biochars from Different Feedstocks and Pyrolysis Temperatures. *J. Anal. Appl. Pyrolysis* **2013**, *102*, 137–143. [CrossRef]
30. Vikash Kumar, K.; Sivasankara Raju, R. Statistical Modeling and Optimization of Al-MMCs Reinforced with Coconut Shell Ash Particulates. In *Innovative Product Design and Intelligent Manufacturing Systems*; Deepak, B.B.V.L., Parhi, D., Jena, P.C., Eds.; Springer: Singapore, 2020; pp. 703–712.

31. Saletnik, B.; Zaguła, G.; Bajcar, M.; Tarapatsky, M.; Bobula, G.; Puchalski, C. Biochar as a Multifunctional Component of the Environment—A Review. *Appl. Sci.* **2019**, *9*, 1139. [[CrossRef](#)]
32. Lassoued, N.; Bilal, E.; Rejeb, S.; Guénole-Bilal, I.; Khelil, N.; Rejeb, M.N.; Gallice, F. Behavior Canola (*Brassica Napus*) Following a Sewage Sludge Treatment. *Carpathian J. Earth Environ. Sci.* **2013**, *8*, 155–165.
33. Adachi, A.; Ouadrhiri, F.E.; Kara, M.; El Manssouri, I.; Assouguem, A.; Almutairi, M.H.; Bayram, R.; Mohamed, H.R.H.; Peluso, I.; Eloutassi, N.; et al. Decolorization and Degradation of Methyl Orange Azo Dye in Aqueous Solution by the Electro Fenton Process: Application of Optimization. *Catalysts* **2022**, *12*, 665. [[CrossRef](#)]
34. Zahoor, M.; Wahab, M.; Salman, S.M.; Sohail, A.; Ali, E.A.; Ullah, R. Removal of doxycycline from water using Dalbergia sissoo waste biomass based activated carbon and magnetic oxide/activated bioinorganic nanocomposite in batch adsorption and adsorption/membrane hybrid processes. *Bioinorg. Chem. Appl.* **2022**. [[CrossRef](#)]
35. Cychosz, K.A.; Guillet-Nicolas, R.; García-Martínez, J.; Thommes, M. Recent Advances in the Textural Characterization of Hierarchically Structured Nanoporous Materials. *Chem. Soc. Rev.* **2017**, *46*, 389–414. [[CrossRef](#)] [[PubMed](#)]
36. Ayiania, M.; Carbajal-Gamarra, F.M.; Garcia-Perez, T.; Frear, C.; Suliman, W.; Garcia-Perez, M. Production and Characterization of H₂S and PO₄³⁻ Carbonaceous Adsorbents from Anaerobic Digested Fibers. *Biomass Bioenergy* **2019**, *120*, 339–349. [[CrossRef](#)]
37. Xu, X.; Huang, H.; Zhang, Y.; Xu, Z.; Cao, X. Biochar as Both Electron Donor and Electron Shuttle for the Reduction Transformation of Cr(VI) during Its Sorption. *Environ. Pollut.* **2019**, *244*, 423–430. [[CrossRef](#)] [[PubMed](#)]
38. Martin, M.J.; Balaguer, M.D.; Rigola, M. Feasibility of Activated Carbon Production from Biological Sludge by Chemical Activation with ZnCl₂ and H₂SO₄. *Environ. Technol.* **1996**, *17*, 667–671. [[CrossRef](#)]
39. Ogasawara, S.; Kuroda, M.; Wakao, N. Preparation of Activated Carbon by Thermal Decomposition of Used Automotive Tires. Available online: <https://pubs.acs.org/doi/pdf/10.1021/ie00072a030> (accessed on 22 June 2022).